AIP | Applied Physics Letters

Atmospheric plasma jet array in parallel electric and gas flow fields for three-dimensional surface treatment

Z. Cao, J. L. Walsh, and M. G. Kong

Citation: Appl. Phys. Lett. **94**, 021501 (2009); doi: 10.1063/1.3069276
View online: http://dx.doi.org/10.1063/1.3069276
View Table of Contents: http://apl.aip.org/resource/1/APPLAB/v94/i2
Published by the American Institute of Physics.

Related Articles

Effect of near atmospheric pressure nitrogen plasma treatment on Pt/ZnO interface
J. Appl. Phys. 112, 116104 (2012)

Momentum transfer and flow induction in a dielectric barrier discharge plasma actuator
AIP Advances 2, 042150 (2012)

Investigation of plasma-doped fin structure and characterization of dopants by atom probe tomography
Appl. Phys. Lett. 101, 213113 (2012)

Adjustment of ablation shapes and subwavelength ripples based on electron dynamics control by designing femtosecond laser pulse trains
J. Appl. Phys. 112, 103103 (2012)

Plasma diagnostics of low pressure high power impulse magnetron sputtering assisted by electron cyclotron wave resonance plasma
J. Appl. Phys. 112, 093305 (2012)

Additional information on Appl. Phys. Lett.

Journal Homepage: http://apl.aip.org/
Journal Information: http://apl.aip.org/about/about_the_journal
Top downloads: http://apl.aip.org/features/most_downloaded
Information for Authors: http://apl.aip.org/authors

ADVERTISEMENT

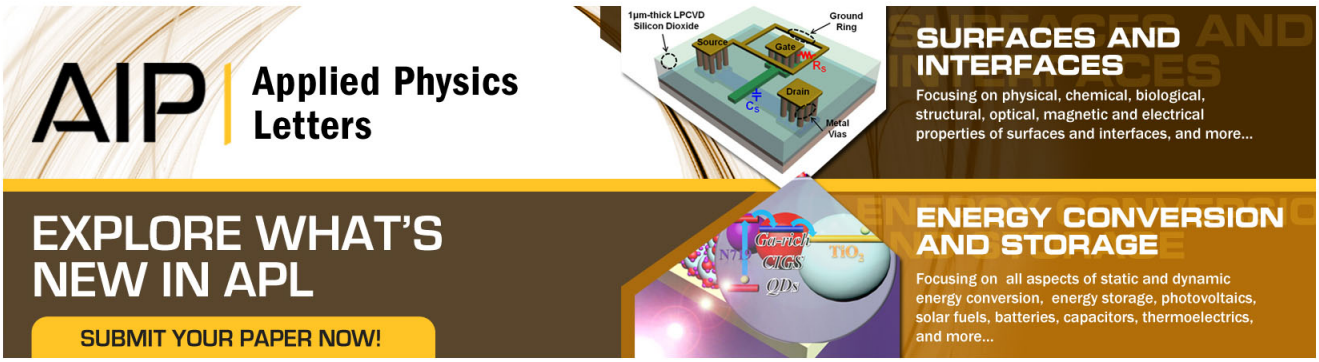

Downloaded 05 Jan 2013 to 128.148.252.35. Redistribution subject to AIP license or copyright; see http://apl.aip.org/about/rights_and_permissions

Atmospheric plasma jet array in parallel electric and gas flow fields for three-dimensional surface treatment

Z. Cao, J. L. Walsh, and M. G. Kong[a)]
Department of Electronic and Electrical Engineering, Loughborough University, Leices LE11 3TU, United Kingdom

(Received 19 August 2008; accepted 16 December 2008; published online 13 January 2009)

This letter reports on electrical and optical characteristics of a ten-channel atmospheric pressure glow discharge jet array in parallel electric and gas flow fields. Challenged with complex three-dimensional substrates including surgical tissue forceps and sloped plastic plate of up to 15°, the jet array is shown to achieve excellent jet-to-jet uniformity both in time and in space. Its spatial uniformity is four times better than a comparable single jet when both are used to treat a 15° sloped substrate. These benefits are likely from an effective self-adjustment mechanism among individual jets facilitated by individualized ballast and spatial redistribution of surface charges. © *2009 American Institute of Physics*. [DOI: 10.1063/1.3069276]

Enjoying an exponential growth in their applications,[1] atmospheric pressure glow discharge (APGD) jets offer excellent plasma stability in the upstream electrode region while enabling rich reaction chemistry with downstream introduction of reactive gases. Spatial separation of their generation from their application regions is beneficial for APGD jets to achieve better application efficiency than APGD sustained between parallel-plate electrodes.[2] However APGD jets typically cover only a few mm^2 and as such are too small for large-scale applications such as surface coating, deposition, and cleaning. An obvious solution is to group many APGD jets together to form an array of longer length scale. Indeed, both microhollow cathode discharges[3] and microcavity discharges[4] have been operated in an array. Using a pin-in-hole configuration, millimeter APGD sources have also been arrayed up to form a 4×4 cm^2 device.[5] A common feature of these APGD arrays is that they are intended for photonics applications for which high electron density of 10^{13}–0^{16} cm^{-3} is important.[3–5] This favors small electrode gaps with which to enhance electric field and confine each plasma, and the spatial plasma confinement makes it difficult to use these APGD arrays directly for active downstream chemistry. Similar difficulties are present for dc or microwave plasma torch array developed for plasma stealth and plasma-aided ignition,[6] both of which require high electron density and favor spatial confinement of individual plasmas. Improvisation is possible with these APGD arrays by adding a second power supply to drag out confined plasmas to downstream,[7] thus making them more amendable for surface processing applications. However, it is far more desirable to develop APGD jet arrays with one power supply and from a single-jet configuration directly for downstream chemistry. This approach has been shown to be viable,[8,9] although without addressing several key issues such as spatial and temporal jet-to-jet variation and the role of ballast. In this letter, we report a study of a ten-jet array with its electrical and optical characterization and with its ability to treat three-dimensional (3D) surfaces.

Of many different single-jet configurations,[8–13] we choose a dielectric tube wrapped with a ring electrode and through which to flow the carrier gas. Each jet may be operated with or without a downstream ground electrode. The electric field is largely in the axial direction and is parallel to the gas flow field, and so each jet is a linear-field device.[14] Figure 1(a) shows the schematic of the ten-jet array housed in an acrylic cassette having each jet compartment constructed in a tubular unit with individual ballast and individual gas feed. Each tubular unit consists of a glass tube of 1.5 mm inner diameter inside a concentric copper tube as the powered electrode, and the entire array device is 3.2 cm in width from the first to the last jet. The flow rate of the helium gas is 4 SLM (SLM stands for standard liters per minute) or 37.7 m/s for each tube, well within the laminar limit. Each ballast has a resistance of 510 kΩ, and the excitation frequency is fixed at 30 kHz. Figures 1(b) and 1(c) are images taken with an Olympus digital camera of the ten-jet APGD array with a screwdriver and a surgical tissue forceps, respectively, as the ground electrode. It is clear that all ten plasma jets are ignited against very different 3D substrates even when different jets in Fig. 1(c) intercept the metallic forceps at very different nozzle-to-forceps distances. This indicates an effective self-adjustment mechanism among individual jets in the array, achieved by individualized ballast

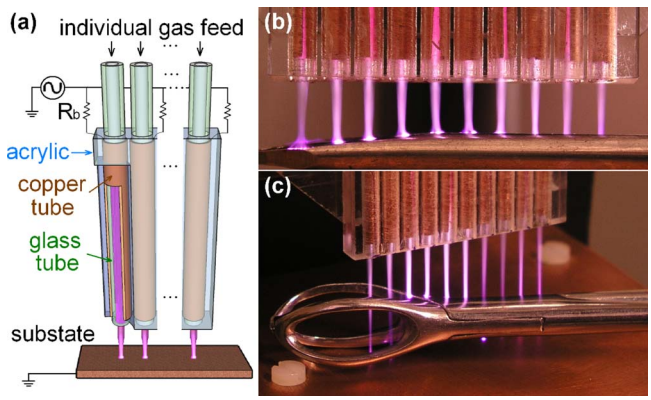

FIG. 1. (Color online) (a) Schematic of a ten-jet atmospheric plasma array with individual ballasts, (b) its image with a screwdriver as the substrate, and (c) its image with a surgical tissue forceps as the substrate.

a)Author to whom correspondence should be addressed. Electronic mail: m.g.kong@lboro.ac.uk.

 © 2009 American Institute of Physics

Downloaded 05 Jan 2013 to 128.148.252.35. Redistribution subject to AIP license or copyright; see http://apl.aip.org/about/rights_and_permissions

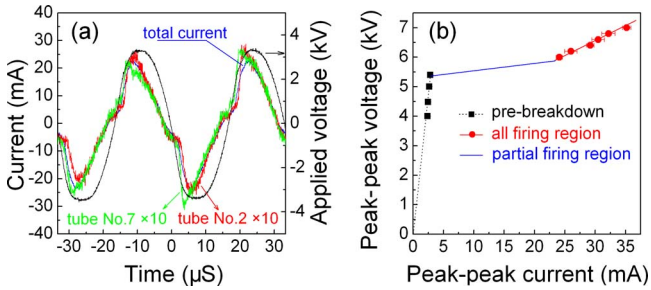

FIG. 2. (Color online) (a) Time traces of the applied voltage, the total discharge, and two individual jet currents; (b) the total current dependence of the applied voltage. The substrate is a 10° sloped PVC substrate.

and possibly by spatial redistribution of surface charges on the acrylic cassette also. It is worth mentioning that all APGD jets fire only when each jet is individually ballasted. The benefit of individualized ballast is similar to that for other high-pressure discharge arrays.[3–5] The above discussion demonstrates a clear robustness of the APGD array for treating intricate metallic objects.

It is worth noting the sharp contrast between the gradual surface profile of the screwdriver and the convoluted structure of the forceps in Fig. 1, highlighting the considerable potential of the APGD jet array for treating massively 3D substrates. The latter is an important indicator of the APGD jet array as a platform tool for sterilization of diverse surgical instruments and medical devices.[15] The APGD jet array reported here is 3.2 cm wide and is intended for characterization study. A larger 30-jet array of 11 cm wide and driven by a single power supply has been developed in our laboratory for application studies and this illustrates the scalability of the jet array configuration for large-scale processing applications.

To demonstrate directly its capability for treating 3D surfaces, the APGD jet array is characterized using a sloped polyvinyl chloride (PVC) plate as a 3D substrate model. Figure 2(a) shows traces of the applied voltage, the total current, and the individual currents flowing through the second and seventh jets, when the PVC plate is sloped at 10° with the shortest and longest nozzle-substrate distances being 1.0 and 1.6 cm, respectively. The individual currents are multiplied by 10 (the number of the jets) to allow for direct comparison to the total current, and they are used as an example of the ten individual currents without compromising the clarity of Fig. 2(a). The waveform of the total current is seen to map very well onto the waveforms of the two individual currents, suggesting that all ten plasma jets fire simultaneously. All current and voltage curves in Fig. 2(a) are free from any obvious spikes, indicating a streamer-free and glow-like character of the jet array. Relationship of the peak-to-peak current and voltage is shown in Fig. 2(b), revealing a regime immediately after gas breakdown during which not all jets are ignited. With increasing applied voltage, more plasma jets start to fire and the total current grows. This regime is similar to the normal mode of the glow discharge. After the peak-to-peak applied voltage is raised to 6.0 kV, a second regime with all jets firing appears as shown in Fig. 2(b). The APGD jet array has positive differential impedance in this second regime and may operate in the abnormal glow mode. Even with positive differential impedance, not all ten jets could fire at the same time if they were first connected together and then connected to a single ballast. This is different

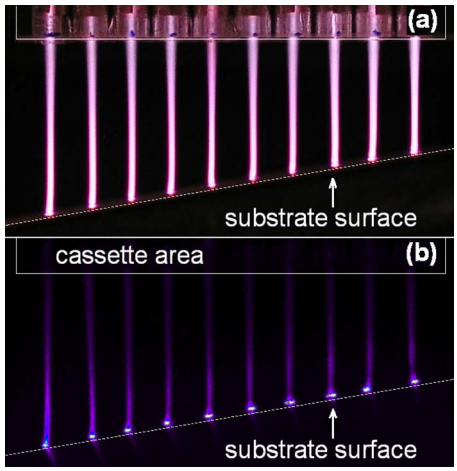

FIG. 3. (Color online) Images of the APGD jet array onto a 10° sloped PVC substrate with exposure times of (a) 1/15 s and (b) 10 ns.

from the case of a 2×2 microhollow cathode discharge array for which ballast resistors were found unnecessary when the differential impedance was positive.[3] The role of individualized ballast is critical in the APGD jet array of Fig. 1 and is likely to have facilitated an in-built self-adjustment mechanism in achieving synchronized operation.

While the near identical time dependences of the total and individual currents in Fig. 2(a) offer a strong indication of synchronized firing of all individual jets, the most direct evidence of the jet-to-jet uniformity would need to be provided from nanosecond exposure imaging. Setting the slope of the PVC plate at 10° and the peak-to-peak applied voltage at 7 kV, two images of the jet array were taken with exposure time of 1/15 s in Fig. 3(a) and of 10 ns in Fig. 3(b) (using an Andor DH 720 iCCD camera). Clearly, all ten jets fire simultaneously, confirming excellent temporal jet-to-jet uniformity. Repeated experiments at different substrate slopes of up to 15° have confirmed that synchronized operation and excellent temporal jet-to-jet uniformity of the APGD jet array are maintained over a wide operating range.

Light intensity of individual jets at the substrate surface appears to be similar to each other in Fig. 3(b); however, it is limited to the visible range of 400–700 nm outside which many application-significant lines lie, for example, the atomic oxygen lines at 777 and 844 nm, helium line at 706 nm, and nitrogen and OH lines in the 300–400 nm band. To overcome this and relate directly to reaction chemistry, an Andor spectrometer was used to measure wavelength-integrated emission intensity from 200 to 1000 nm. Spatial separation of the light emission of one jet from that of other jets was achieved using the light-isolation device shown in Fig. 4(a). Given the distance between two adjacent jets being 3.5 mm, light density measurement via the isolation device is made within 3.5 mm either side of the location of a firing plasma jet in dark ambience. Figure 4(b) shows that the light of a firing plasma jet collected by the isolation device falls to the background noise level within 1.75 mm away from the jet location, in other words, at the midpoint to an adjacent jet of the jet array. This suggests that light emission from any source outside the 1.75 mm radius, either the remaining plasma jets in the array or otherwise, is blocked out by the isolation device, thus achieving effective spatial selectivity of optical emission from different jets.

Downloaded 05 Jan 2013 to 128.148.252.35. Redistribution subject to AIP license or copyright; see http://apl.aip.org/about/rights_and_permissions

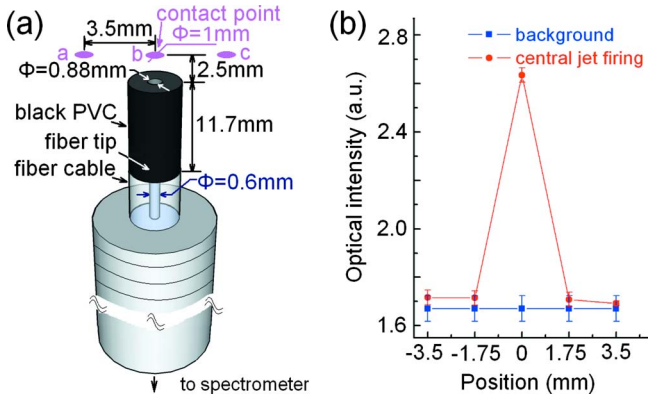

FIG. 4. (Color online) (a) Schematic of a light-isolation device and its integration to the light-collecting fiber cable to a spectrometer. Labels a, b, and c mark the substrate-interception points of three consecutive plasma jets in the jet array. (b) Optical emission of one firing plasma jet measured by scanning the light-isolation device over 3.5 mm either side of the jet.

The light-isolation device is used to establish the spatial jet-to-jet uniformity of the APGD jet array in comparison to that of a single jet which needs to scan when treating a large surface area. Although an APGD jet array requires much less scanning, possible fabrication variation from one jet to another may affect the uniformity of its treated surface. To compare their difference, we consider a surface-scanning single jet with a stationary jet array. Using the isolation device, the wavelength-integrated light intensity of each of the ten jets of the APGD jet array was measured at their interception point by a sloped PVC substrate, and then compared to those of the single jet as the latter scans across the same substrate points. Results are shown in Fig. 5, with the emission intensity of the jet array in Fig. 5(a) exhibiting a much better spatial jet-to-jet uniformity than that of the single-jet

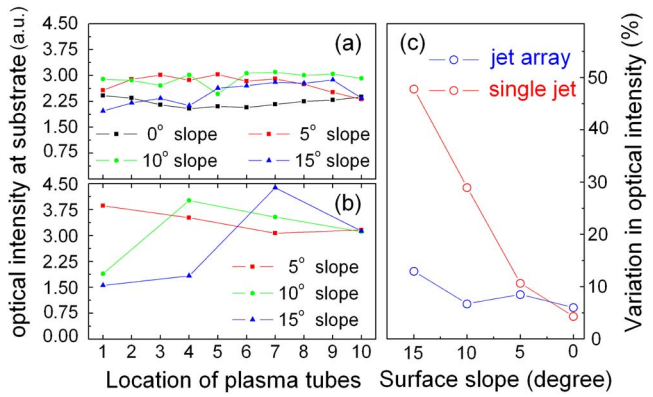

FIG. 5. (Color online) Optical emission from (a) each of the ten jets in the jet array and from (b) a scanning single jet, as well as (c) the spatial variation in optical emission as a function of the slope of the PVC substrate plate for the jet array (blue) and for the single jet (red).

in Fig. 5(b), particularly at substrate slopes above 5°. In the single-jet case, variation in optical intensity across the sampled surface points is seen in Fig. 5(c) to increase from 4.0% at 0° slope to 48% at 15° slope. By contrast, the jet array has much smaller intensity variation from 6% at 0° slope to 12% at 15° slope. This demonstrates an excellent spatial jet-to-jet uniformity of the APGD jet array, a factor of 4 (=48%/12%) better than that of the single jet in the 15° slope case. The jet array covers about ten times more surface area than a single-jet at any given time, and this can be easily translated into a factor of 10 reduction in the processing time.

In summary, electrical and optical characterizations of an APGD jet array have been used to demonstrate its robust temporal and spatial jet-to-jet uniformity against complex 3D substrates. On sloped substrates of 5°–15°, the jet array has consistently better spatial uniformity than its single jet counterpart. These highlight a high-level consistency of the APGD jet array in maintaining its plasma physical and chemical characters when treating vastly 3D objects. This is largely resulted from a self-adjustment mechanism among individual jets facilitated by individualized ballast and possibly also by spatial redistribution of surface charges. The jet array behaves like one integrated plasma with effective internal feedback among individual jets and behaves like a glow discharge with operation regimes resembling the normal and abnormal modes of the glow discharge. The plume length of the APGD jet array is typically above 2 cm in the free-burning mode, similar to that of reported single jets and well suited for treating 3D structures on a large scale.

[1]K. H. Becker, K. H. Schoenbach, and J. G. Eden, J. Phys. D **39**, R55 (2006).
[2]X. T. Deng, J. J. Shi, and M. G. Kong, IEEE Trans. Plasma Sci. **34**, 1310 (2006).
[3]K. H. Schoenbach, R. Verhappen, T. Tessnow, and F. E. Peterkin, Appl. Phys. Lett. **68**, 13 (1996).
[4]P. von Allmen, D. J. Sadler, C. Jensen, N. P. Ostrom, S. T. McCain, B. A. Vojak, and J. G. Eden, Appl. Phys. Lett. **82**, 4447 (2003).
[5]T. Sakaguchi, O. Sakai, and K. Tachibana, J. Appl. Phys. **101**, 073305 (2007).
[6]E. Koretzky and S. P. Kuo, Phys. Plasmas **5**, 3774 (1998).
[7]Y.-B. Guo and F. C.-N. Hong, Appl. Phys. Lett. **82**, 337 (2003).
[8]Z. Hubicka, M. Cada, M. Sicha, A. Churpita, P. Pokorny, L. Soukup, and L. Jastrabik, Plasma Sources Sci. Technol. **11**, 195 (2002).
[9]R. Foest, E. Kindel, A. Ohl, M. Stieber, and K.-D. Weltmann, Plasma Phys. Controlled Fusion **47**, B525 (2005).
[10]A. Schutze, J. Y. Jeong, S. E. Babayan, J. Park, G. S. Selwyn, and R. F. Hicks, IEEE Trans. Plasma Sci. **26**, 1685 (1998).
[11]M. Teschke, J. Kedzierski, E. G. Finantu-Dinu, D. Korzec, and J. Engemann, IEEE Trans. Plasma Sci. **33**, 310 (2005).
[12]J. L. Walsh, J. J. Shi, and M. G. Kong, Appl. Phys. Lett. **88**, 171501 (2006).
[13]X. Lu and M. Laroussi, J. Appl. Phys. **100**, 063302 (2006).
[14]J. L. Walsh and M. G. Kong, Appl. Phys. Lett. **93**, 111501 (2008).
[15]X. T. Deng, J. J. Shi, and M. G. Kong, J. Appl. Phys. **101**, 074701 (2007).

Downloaded 05 Jan 2013 to 128.148.252.35. Redistribution subject to AIP license or copyright; see http://apl.aip.org/about/rights_and_permissions